Celest Mech Dyn Astr (2009) 103:79–103
DOI 10.1007/s10569-008-9169-y

ORIGINAL ARTICLE

Earth–Moon Weak Stability Boundaries in the restricted three and four body problem

Daniele Romagnoli · Christian Circi

Received: 22 February 2008 / Revised: 29 October 2008 / Accepted: 5 November 2008 /
Published online: 12 December 2008
© Springer Science+Business Media B.V. 2008

Abstract This work deals with the structure of the lunar Weak Stability Boundaries (WSB) in the framework of the restricted three and four body problem. Geometry and properties of the escape trajectories have been studied by changing the spacecraft orbital parameters around the Moon. Results obtained using the algorithm definition of the WSB have been compared with an analytical approximation based on the value of the Jacobi constant. Planar and three-dimensional cases have been studied in both three and four body models and the effects on the WSB structure, due to the presence of the gravitational force of the Sun and the Moon orbital eccentricity, have been investigated. The study of the dynamical evolution of the spacecraft after lunar capture allowed us to find regions of the WSB corresponding to stable and safe orbits, that is orbits that will not impact onto lunar surface after capture. By using a bicircular four body model, then, it has been possible to study low-energy transfer trajectories and results are given in terms of eccentricity, pericenter altitude and inclination of the capture orbit. Equatorial and polar capture orbits have been compared and differences in terms of energy between these two kinds of orbits are shown. Finally, the knowledge of the WSB geometry permitted us to modify the design of the low-energy capture trajectories in order to reach stable capture, which allows orbit circularization using low-thrust propulsion systems.

Keywords Weak Stability Boundaries · Four body problem · Low-energy transfer

1 Introduction

Low energy interplanetary transfers have been widely studied in the last twenty years and a large number of publications are available in the literature (Belbruno 1987, 2004; Belbruno and Miller 1990; Kawaguchi et al. 1995; Koon et al. 2000, 2001). Particularly, these kinds of

D. Romagnoli · C. Circi (✉)
Scuola di Ingegneria Aerospaziale, Università di Roma "La Sapienza", Via Eudossiana 16,
00184 Rome, Italy
e-mail: christian.circi@uniroma1.it

transfers roused interest in designing lunar trajectories. In this way, in fact, it is possible to save up to 15% propellant mass compared with classic Hohmann transfers. Many different ways have been proposed for the design (Belbruno 1987; Belbruno et al. 1993; Bellò et al. 2000; Koon et al. 2001; Circi and Teofilatto 2001), but all these techniques use particular space regions, called Weak Stability Boundaries. Belbruno (2004) suggested an algorithm definition of WSB and presented their geometry for the Earth–Moon system in the planar case, in terms of eccentricity, periselenium altitude and Jacobi constant of the spacecraft osculating initial orbit. Using the Belbruno definition, Garcia and Gomez (2007) showed the WSB in the framework of the circular restricted three body problem and located stable and unstable points in the plane of motion of the two primaries of motion. In this paper, the WSB are studied using three and four body models, investigating the configuration of the stable and unstable regions in both planar and three-dimensional cases. Stable regions are compared with the sphere of influence and are used to design low-energy transfers. In Sect. 2, the three and four body models used in simulations are discussed. Section 3 deals with the definition and characteristics of the WSB in terms of capture conditions. Numerical results are then compared with an analytical approximation based on the value of the Jacobi constant. In Sect. 4, the definition of the WSB is extended to the three-dimensional case. In Sect. 5 the dynamics after capture is studied, in order to locate safe regions inside the WSB, that is conditions that avoid impacts with the lunar surface. Finally, Sect. 6 deals with lunar WSB transfers in terms of capture periselenium altitude and the maps obtained are used to design lunar transfers with stable behavior.

2 Equation of motion

In this section, the restricted three and four body models used to study the WSB structure are discussed. Consider two masses m_1 and m_2, the so called primaries of motion, moving around their common center of mass and satisfying the condition $m_1 > m_2$. Let's introduce a third body of negligible mass m, so that $m \ll m_2 < m_1$, moves in the gravity field produced by the two primaries. The motion of the third body is studied in a rotating reference frame whose origin is located on the center of mass of the primaries, the x axis is along the line between the primaries, the z axis is normal to the plane of motion of the primaries and the y axis forms a right hand reference frame. If the two primaries move on a circular orbit around their common center of mass, the model is referred to as the Circular Restricted Three Body Problem (CRTBP), whereas if the two massive bodies move on elliptic orbits the model is called the Elliptic Restricted Three Body Problem (ERTBP). In the CRTBP, the equations of motion for the mass m can be expressed in terms of the second derivatives of a potential function $\Omega_3(x, y, z)$ defined as:

$$\Omega_3(x, y, z) = \frac{1}{2}(x^2 + y^2) + \frac{1-\mu}{r_1} + \frac{\mu}{r_2} + \frac{1}{2}\mu(1-\mu) \tag{1}$$

where $\mu = \frac{m_2}{m_1+m_2}$ is the mass parameter of the system, $r_1 = \sqrt{(x+\mu)^2 + y^2 + z^2}$ and $r_2 = \sqrt{(x+\mu-1)^2 + y^2 + z^2}$ the distances of the third body from m_1 and m_2 and $\frac{1}{2}\mu(1-\mu)$ is a constant for the potential, respectively. Note that the term $\frac{1}{2}\mu(1-\mu)$, which does not modify the equations of motion, is usually introduced in the literature in order to have a more symmetrical potential function (Szebehely 1967). Obtaining the second derivatives from (1),

the equations of motion can be written as (Wie 2000):

$$\begin{cases} \ddot{x} - 2\dot{y} - x = -\dfrac{(1-\mu)(x+\mu)}{r_1^3} - \dfrac{\mu(x+\mu-1)}{r_2^3} \\ \ddot{y} + 2\dot{x} - y = -\left(\dfrac{1-\mu}{r_1^3} + \dfrac{\mu}{r_2^3}\right) y \\ \ddot{z} = -\left(\dfrac{1-\mu}{r_1^3} + \dfrac{\mu}{r_2^3}\right) z \end{cases} \tag{2}$$

In the ERTBP, the two primaries move on elliptic orbits around their common center of mass. Hence, the instantaneous distance between m_1 and m_2 and the angular rate of the reference frame vary in time. In this case, the equations of motion for the third body are (Wie 2000):

$$\begin{cases} \ddot{x} - 2\omega\dot{y} = \dot{\omega} y + \omega^2 x - \dfrac{(1-\mu)}{r_1^3}(x - x_1) - \dfrac{\mu}{r_2^3}(x - x_2) \\ \ddot{y} + 2\omega\dot{x} = -\dot{\omega} x + \omega^2 y - \left(\dfrac{1-\mu}{r_1^3} + \frac{\mu}{r_2^3}\right) y \\ \ddot{z} = -\left(\dfrac{1-\mu}{r_1^3} + \dfrac{\mu}{r_2^3}\right) z \end{cases} \tag{3}$$

where ω is the actual angular rate of the reference frame, x_1 and x_2 are the coordinates along the x axis of the primaries and r_1 and r_2 are the instantaneous distances between the spacecraft and the Earth and the spacecraft and the Moon, respectively, defined as $r_1^2 = (x - x_1)^2 + y^2 + z^2$ and $r_2^2 = (x - x_2)^2 + y^2 + z^2$. Moreover, the motion of the third body is studied using dimensionless quantities:

- The unit of distance is equal to the mean distance between the primaries;
- The unit of mass is equal to the sum of the masses of the primaries;
- The unit of time is such that the period of m_2 about m_1 is equal to 2π.

The next model introduced is the Bicircular Restricted Four Body Problem (BRFBP). Compared with the case of the CRTBP, in which the Earth and the Moon move on circular orbits around the system center of mass, the BRFBP adds the presence of the Sun, rotating around the Earth–Moon system with a constant radius ρ and constant relative angular rate ω_s. The equations of motion can still be obtained using a potential function $\Omega_4 = \Omega_4(x, y, z)$ including the terms related to the Sun:

$$\Omega_4(x, y, z) = \Omega_3(x, y, z) + \frac{m_S}{r_3} - \frac{m_S}{\rho^2}(x \cos\varphi(t) + y \sin\varphi(t)) \tag{4}$$

where m_s is the mass of the Sun, $r_3 = \sqrt{(x - \rho\cos\varphi)^2 + (y - \rho\sin\varphi)^2 + z^2}$ is the distance between the spacecraft and the Sun and $\varphi = \bar{\varphi}(t) + \varphi_0$ is the phase angle between the Sun and the Earth–Moon direction (Figs. 23, 25). Hence, the equations of motion for the spacecraft can be written as (Yagasaki 2004):

$$\begin{cases} \ddot{x} - 2\dot{y} = \dfrac{\partial \Omega_4}{\partial x} \\ \ddot{y} + 2\dot{x} = \dfrac{\partial \Omega_4}{\partial y} \\ \ddot{z} = \dfrac{\partial \Omega_4}{\partial z} \\ \dot{\vartheta} = \omega_s \end{cases} \tag{5}$$

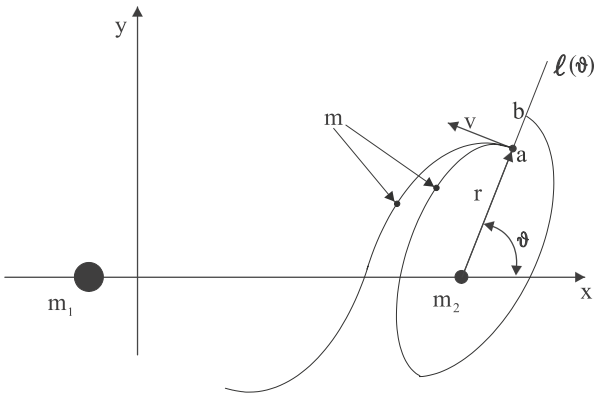

Fig. 1 Algorithmic definition of the WSB

The bicircular model is a good approximation for the Earth–Moon–Sun system. The eccentricity of the Earth's orbit about the Sun ($e_{\text{earth}} = 0.016$) and that of the Moon's orbit around the Earth ($e_{\text{moon}} = 0.054$), are, in fact, very small and the lunar orbital plane is inclined by only 5° with respect to the ecliptic plane. The dimensionless characteristic values used in this model are:

- The relative Sun angular rate is set equal to $\omega_s = -0.9251$.
- The distance between the Sun and the Earth–Moon center of mass is set equal to $\rho = 3.8881 \times 10^{12}$.
- The mass of the Sun is set equal to $m_s = 3.289 \times 10^5$.

3 Weak Stability Boundaries

The definition of the Weak Stability Boundaries is based on the following algorithm (Belbruno 2004). Let's introduce two masses m_1 and m_2, so that the condition $m_1 > m_2$ is verified, and a third particle m satisfies the condition $m \ll m_2 < m_1$. In the synodic reference frame introduced in Sect. 2, consider a radial line $l(\vartheta)$ from m_2, defining an angle ϑ with the x axis of the reference frame (Fig. 1).

In order to define the WSB, let's consider all the trajectories of the third body m having origin on the radial line $l(\vartheta)$ and such that:

- The initial velocity vector ($\mathbf{v}$) of the mass m is normal to the radial line in positive (direct) or negative (retrograde) direction with respect to m_2;
- The Keplerian energy of the mass m with respect to the small primary m_2 is negative;
- The eccentricity of the initial osculating orbit of the spacecraft is constant at each variation of the initial point on the radial line $l(\vartheta)$.

The motion of the spacecraft begins at $t = t_0$ on a point 'a', corresponding to the periselenium of the osculating orbit around m_2 with eccentricity e. For any further time, the motion of the third body is stable with respect to m_2 if:

- after leaving the radial line $l(\vartheta)$ the mass m performs a complete revolution around m_2 and crosses again the radial line in a point $b \in l(\vartheta)$, which is generally different from the starting point, with negative or zero Keplerian energy with respect to m_2 without going around m_1.

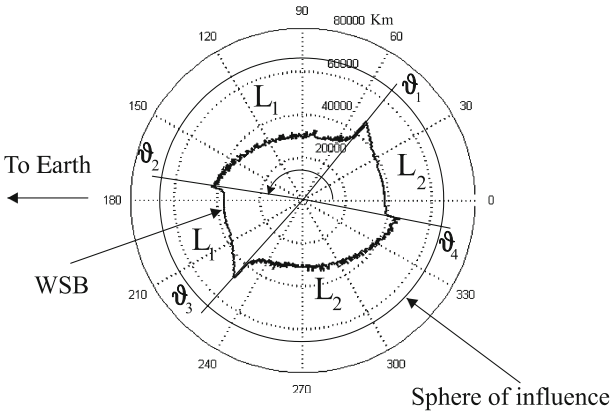

Fig. 2 WSB in Planar Restricted Circular Three Body Problem according to the definition given by Belbruno (with osculating orbit eccentricity $e = 0$)

On the contrary, the motion of the third body is unstable if:

- after leaving the radial line $l(\vartheta)$ the mass m crosses again the direction $l(\vartheta)$ in a point $b \in l(\vartheta)$ without going about m_1, but with positive Keplerian energy with respect to m_2;
- after leaving the radial line $l(\vartheta)$, the third body moves away from m_2 towards m_1 and makes a cycle about m_1 without crossing the radial direction $l(\vartheta)$ or it collides with m_1.

Varying the distance between m and m_2 along the radial line $l(\vartheta)$ with a fixed value of the osculating orbit eccentricity (in example $e = 0$), it is possible to find the values of the radius r and anomaly ϑ which lead to the transition from stable to unstable conditions. Setting r^* as the first radius value for the transition for each value of the anomaly ϑ, according to the definition given by Belbruno, we have:

- stable motion for $r < r^*$
- unstable motion for $r \geqslant r^*$.

In order to compare the lunar WSB with the lunar sphere of influence, it is possible to plot in a polar graph the values of r^* and anomaly ϑ corresponding to the transition between stable and unstable conditions. In the framework of the CRTBP, using $\Delta r = 1{,}000$ km and $\Delta\vartheta = 1^\circ$ as steps for the radius and for the anomaly, the results obtained from numerical simulations with an integrating time of 35 days are shown in Fig. 2.

Figure 2 shows the geometry of the WSB according to the definition given by Belbruno. As illustrated, the WSB have a halved extension compared to the sphere of influence of the Moon. Moreover, the WSB presents four discontinuities identified by the four values of anomaly ϑ_1, ϑ_2, ϑ_3 and ϑ_4. The spacecraft trajectories showed that the discontinuities in $\vartheta_1 = 59.2^\circ$ and $\vartheta_3 = 236.1^\circ$ locate points in which the spacecraft behavior changes globally. In the case of anomaly values $\vartheta < \vartheta_1$, the spacecraft escapes towards the L_2 Lagrangian point, that is towards the outer regions of the Earth–Moon system, while in the case of anomaly $\vartheta > \vartheta_1$ the third body escapes towards the L_1 Lagrangian point, that is towards the inner regions of the Earth–Moon system. The same happens for the discontinuity ϑ_3, where the escape is towards the L_1 Lagrangian point for anomaly values $\vartheta < \vartheta_3$ and towards the L_2 Lagrangian point for anomaly values $\vartheta > \vartheta_3$. Figure 3 shows the four trajectories for these cases.

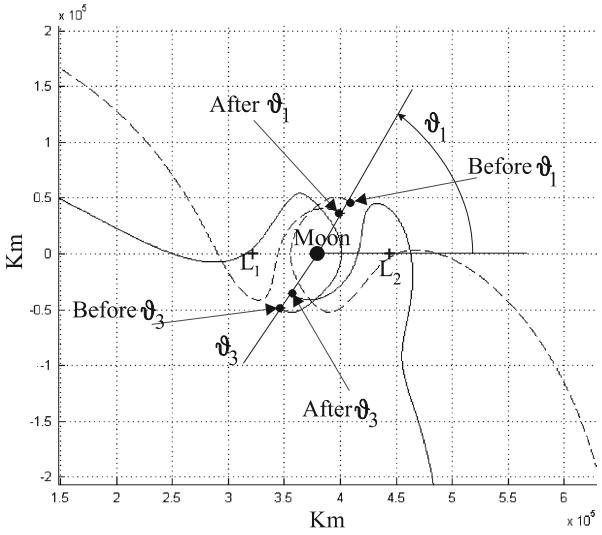

Fig. 3 Different kinds of escape for the discontinuities in $\vartheta = \vartheta_1$ and $\vartheta = \vartheta_3$

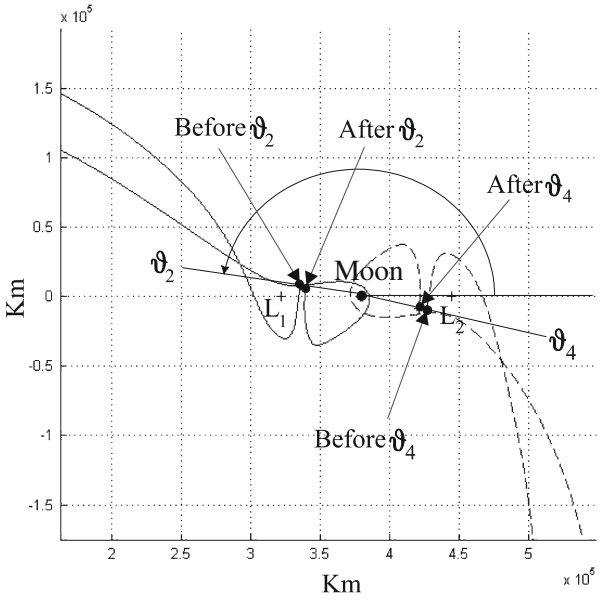

Fig. 4 Different kinds of escapes for the discontinuities in $\vartheta = \vartheta_2$ and $\vartheta = \vartheta_4$

For anomaly values $\vartheta_2 = 170.6°$ and $\vartheta_4 = 348.1°$ the spacecraft global behavior remains the same, that is the escape is always towards the same Lagrangian point, but different kinds of motion are possible for the same type of escape. Particularly, anomaly values $\vartheta < \vartheta_2$ lead to "direct" escapes towards L_1 so that the spacecraft does not perform any revolution around the Moon, while for anomaly values $\vartheta > \vartheta_2$ the third body performs "indirect" escapes towards L_1, that is the spacecraft makes a complete revolution around m_2 prior to escape. In the case of the discontinuity in ϑ_4 the situation is similar to that described for ϑ_2, but oriented to L_2 (Fig. 4).

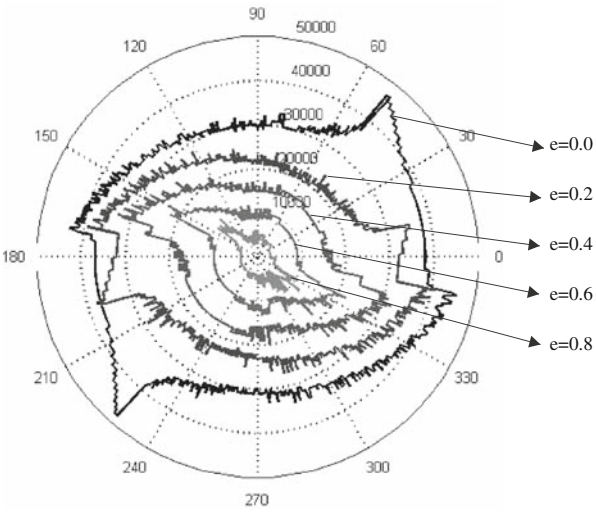

Fig. 5 WSB geometry depending on the spacecraft initial eccentricity

It is easily seen that slight variations in the initial conditions strongly affect the motion of the third body, through both global and local variations of the escape geometry. Besides, slight variations in initial conditions also affect the stability of motion in the vicinity of the WSB. Simulations showed that small increments of the anomaly, of about $\Delta\vartheta \cong 0.1°$, and of the radius, of about $\Delta r \cong 100\,\text{km}$, may cause instability in the motion of the third body, so that the spacecraft moves from an orbit around m_2 to an orbit around m_1. The same procedure, illustrated above, to determine the WSB with $e = 0$ may be followed for different values of the eccentricity. Results are shown in Fig. 5.

As illustrated, for increasing values of the eccentricity e, the stable zone becomes smaller and closer to the Moon, and capture is possible only for low periselenium altitudes. Note that the region closer to the Moon corresponds to capture orbits with low periselenium altitudes and high eccentricities, which are the ones involved in low-energy lunar transfers. The structure and the properties of the WSB can be studied with retrograde (negative) initial velocities of the spacecraft on the osculating orbit. Figure 6 shows the geometry of the WSB for retrograde orbits with different values of the eccentricity.

As illustrated, the behavior of the retrograde WSB for increasing values of the eccentricity of the initial osculating orbit is the same as in the case of positive spacecraft initial velocities: the size of the WSB decreases remarkably, limiting the existence of stable conditions only to a region very close to the Moon. The WSB algorithm definition given above ends when the first stable/unstable transition around m_2 occurs. Actually, numerical simulations showed that, for values of the radius bigger than r^*, multiple transitions occur. Therefore, it is possible to determine a finite number of points r_k^*, with $r_1^* = 0$, such that the stable region can be defined as (Garcia and Gomez 2007):

$$r \in (r_1^*, r_2^*) \cup (r_3^*, r_4^*) \cup (r_5^*, r_6^*) \cup \cdots \cup (r_{k-1}^*, r_k^*) \tag{6}$$

Using this criterion it is possible to draw the new geometry of the lunar WSB in the Earth–Moon system. Figure 7 shows the structure of the WSB within the CRTBP framework and the osculating initial orbit eccentricity set equal to $e = 0$. Note that the colored region indicates the set of stable conditions.

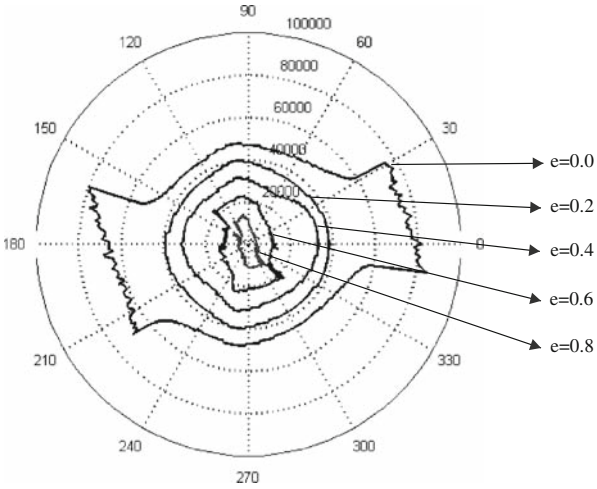

Fig. 6 WSB in the Planar Circular Restricted Three Body Problem and retrograde circular orbits (Belbruno definition)

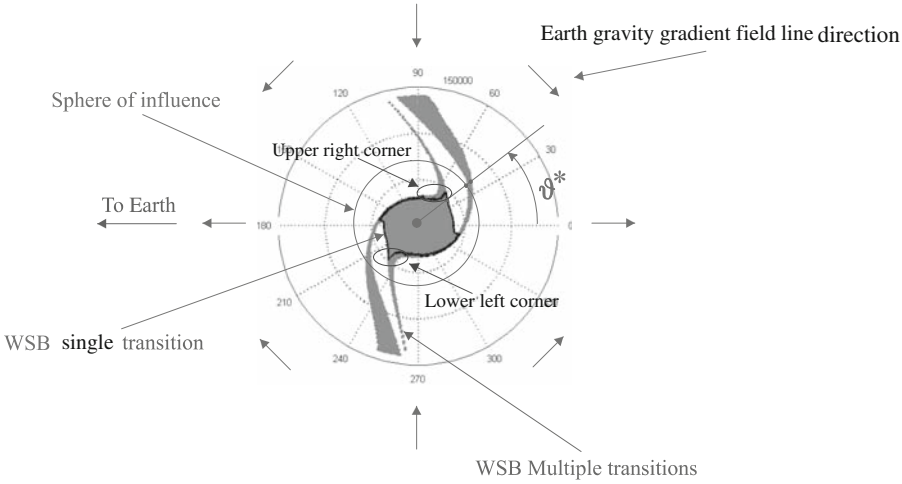

Fig. 7 Comparison between the WSB with single and multiple stable/unstable transitions

As illustrated, four arms appear and, therefore, for a fixed value of the anomaly ϑ there are multiple transitions from stable conditions to unstable conditions, and vice versa. Note that if the WSB obtained with the Belbruno algorithm (black line) is superimposed to that one obtained with the multiple transition algorithm, it is clear that the four arms begin directly in correspondence of the four small peaks identified through the Belbruno definition. Figure 7 shows that for $\vartheta = \vartheta^*$ there are three large scale transitions: stable/unstable, unstable/stable and, again, stable/unstable. Nevertheless, it is important to note that small scale transitions appear in the vicinity of the WSB defined by the Belbruno definition. Particularly, focusing on the region near the two bigger peaks (Figs. 7, 8), it is immediately seen that within a short range in the radius r it is possible to find stable conditions (gray points) very close to the WSB defined by the Belbruno definition (black points).

The same kind of small scale transitions can be easily found in the vicinity of ϑ_3 (Fig. 9).

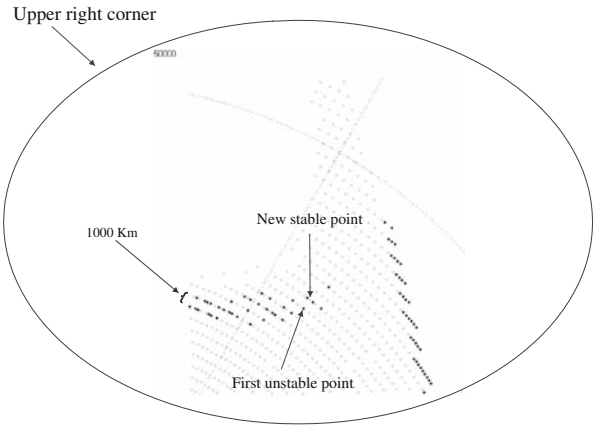

Fig. 8 Small scale stable/unstable transitions in the vicinity of v_1

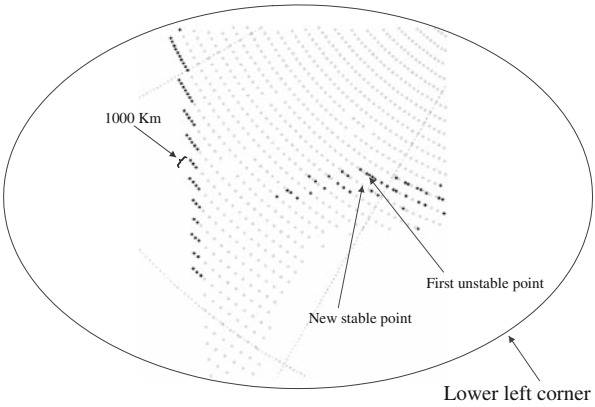

Fig. 9 Small scale stable/unstable transitions in the vicinity of v_3

Stable points identify a region in space, the so called capture zone, corresponding to conditions for the mass m that lead to a stable orbit around the Moon, that is the spacecraft performs at least one complete revolution around the Moon with negative energy. The WSB arms extend perpendicularly to the Earth–Moon direction and may be related to the Earth gravity-gradient. Assuming a direct (positive) direction of the spacecraft initial velocity around the Moon, where the gravity-gradient opposes the motion of the third body subtracting energy from it, there are a greater number of stable points that can be used for captures. This implies that in the $m_1 - m_2$ direction, where the Earth gravity-gradient moves the spacecraft away from the Moon, there are no stable points beyond the lunar sphere of influence. Figure 10 shows the structure of the WSB for different values of the initial osculating orbit eccentricity of the spacecraft. In particular the cases $e = 0$, $e = 0.2$ and $e = 0.4$ are illustrated.

The global geometry does not change a lot for increasing values of the eccentricity, and it is clear that the most impressive change is the reduction of the stable zone close to the Moon. Besides, if the eccentricity increases, the plot of the WSB rotates clockwise, moving the starting points of the arms, which tend to collapse reducing the unstable zone between them and forming a single structure. The same approach can be followed using retrograde conditions for the initial velocity of the spacecraft on the osculating orbit. Figure 11 compares

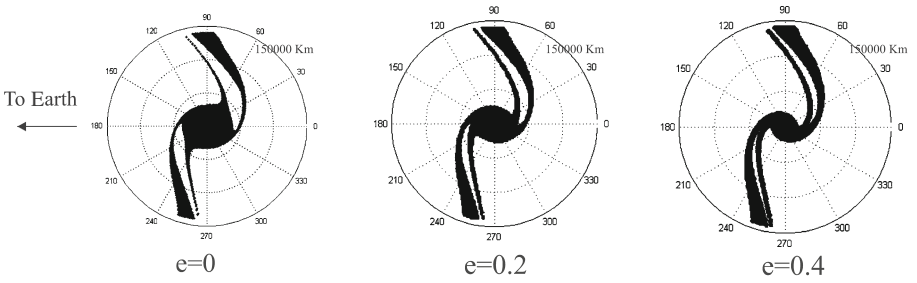

Fig. 10 WSB structure for different values of the initial spacecraft eccentricity

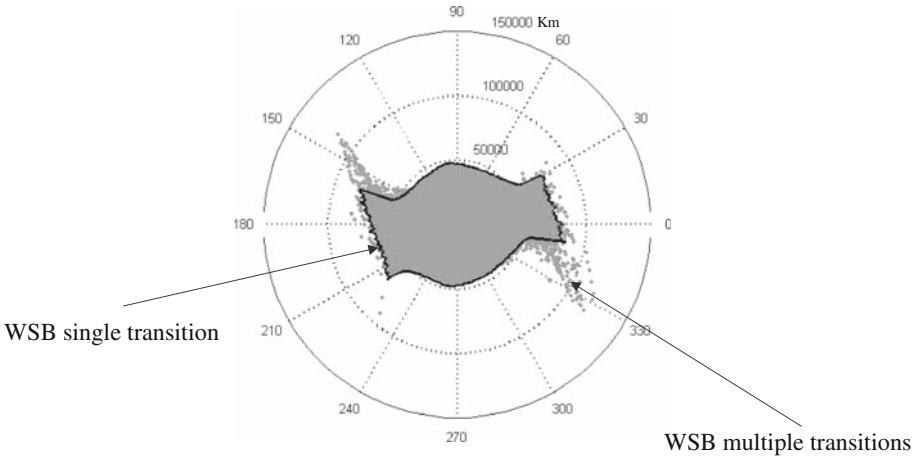

Fig. 11 Comparison between WSB geometry single and multiple transition definition and negative initial velocity

the WSB structure with initial negative velocity obtained with the Belbruno definition (black line) against to the WSB obtained using the multiple transition definition (gray points).

As showed in the case of positive velocities, when comparing the WSB obtained with the Belbruno definition against that one with multiple transitions, large and small scale transitions occur. As previously illustrated, the multiple transition definition allows taking into consideration points which are far away from the Moon. It is also possible to investigate the geometry of the retrograde WSB for different values of the initial eccentricity of the osculating orbit of the spacecraft. Results of this analysis are shown in Fig. 12, where the geometry of the WSB for negative velocities and increasing values of the eccentricity of the initial osculating orbit has been determined, with particular attention to the cases $e = 0$, $e = 0.2$ and $e = 0.4$.

Figure 12 shows that as in the case of positive initial (direct) velocity of the spacecraft, the extension of the WSB decreases as the eccentricity of the osculating initial orbit increases. Similarly to the direct case, for high values of the eccentricity e, the WSB is basically bounded to a region close to the Moon, which corresponds to capture orbits with low periselenium. It is important to note that in order to study low–energy lunar transfer (see Sect. 6) direct orbits are of great interest, hence only the WSB related to direct initial conditions will be investigated from now on. Considering a circular initial orbit for the spacecraft, the values of the Jacobi constant are illustrated in Fig. 13.

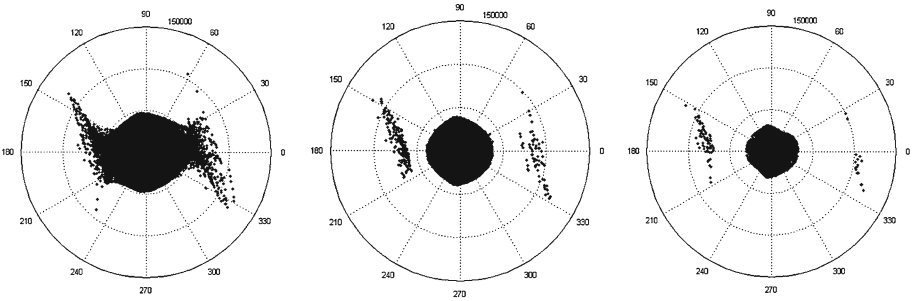

Fig. 12 WSB structure for retrograde initial orbits and different values of the eccentricity of the initial osculating orbit

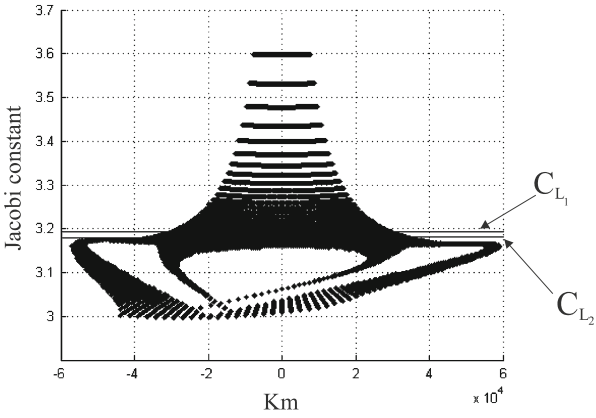

Fig. 13 Jacobi constant for stable points ($e = 0$)

Note that the stable points exist also for Jacobi constant values smaller than that corresponding to the libration points (C_{L_1} and C_{L_2}), that is when the zero velocity curves are fully opened and escapes are possible through both L_1 and L_2. The algorithmic definition of the WSB leads to a numerical representation of this region. Nevertheless, it is possible to obtain an analytical approximation of the WSB geometry in space (r, ϑ) by studying the Jacobi constant in the Earth–Moon system. Belbruno (2004) gives a representation of this analytical approximation in terms of the eccentricity (e), the periselenium (r_p) and the Jacobi constant. In order to compare the numerical solution with the analytical approximation of WSB, it is necessary to express the Jacobi constant in polar coordinates using r and ϑ (Garcia and Gomez 2007):

$$C(r_2, \vartheta, e) = 2\sqrt{\mu(1+e)r_2} - r_2^2 - \frac{\mu(e-1)}{r_2} + \frac{2(1-\mu)}{\sqrt{(r_2\cos\vartheta - 1)^2 + r_2^2\sin^2\vartheta}} + (r_2\cos\vartheta - 1 + \mu)^2 + r_2^2\sin^2\vartheta + \mu(1-\mu) \tag{7}$$

with r_1 and r_2 the distances of the spacecraft from the Earth and the Moon, respectively. Using this expression and fixing the value of the eccentricity of the osculating initial orbit, the values of the Jacobi constant in the Earth–Moon system are evaluated for each different value of distance r and anomaly ϑ. Hence, the analytical approximation of the WSB is obtained sectioning the Jacobi constant surface, given by Eq. 7, with the plane $C = C_{L_2}$. Figure 14 shows the analytical approximation of the lunar WSB and the numerical solution,

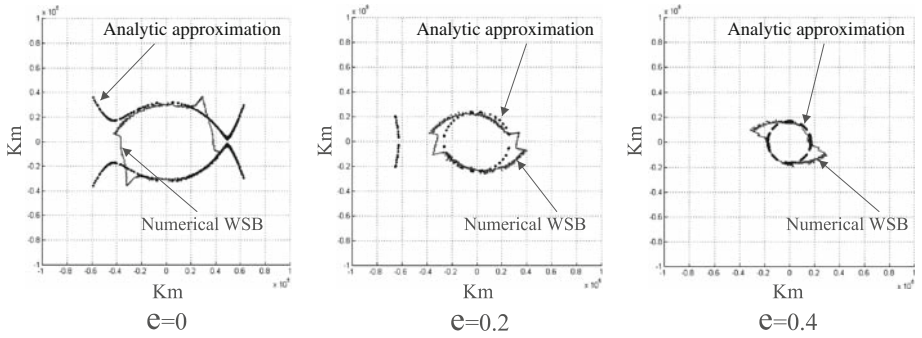

Fig. 14 Comparison between numerical and analytic solutions for the lunar WSB

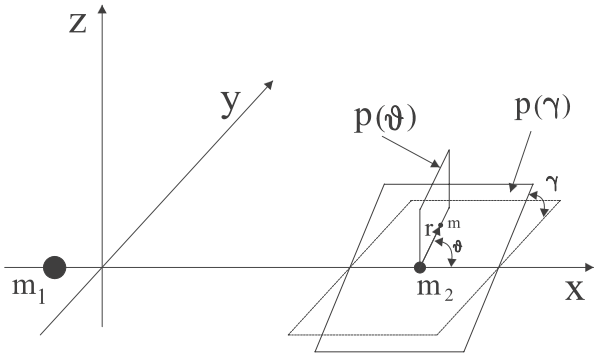

Fig. 15 Planes $p\,(\gamma)$ and $p\,(\vartheta)$ for three-dimensional definition of WSB

considering only the first stable/unstable transition, for different values of the eccentricity of the osculating initial orbit of the spacecraft around the Moon, such as $e = 0$, $e = 0.2$ and $e = 0.4$.

The analytic approximation is a good description of the WSB built considering only the first stable/unstable transition, while in the case of multiple transitions the information about the existence of the arms normal to the Earth–Moon direction is completely lost.

4 WSB: three-dimensional case

In order to study the three-dimensional definition of the WSB, let's consider the case where the initial orbit plane of the third body m does not lie in the plane of motion of the two primaries, but on a plane $p(\gamma)$ rotated by an angle γ around the x axis of the synodic reference frame. Due to the out of plane component of motion, for $t > t_0$ the mass m leaves the plane $p(\gamma)$ and will not cross the radial line $l(\vartheta)$ defined in Sect. 3. Therefore, the motion will always be classified as unstable, according to the stability criterion stated above. For that reason, the radial line $l(\vartheta)$ is substituted by the semi-plane $p(\vartheta)$, normal to the plane $p(\gamma)$ and including m_2 and m (Fig. 15).

Note that it is possible to introduce a similar criterion for motion stability and instability. The motion of the third body m is stable with respect to m_2 if:

- after leaving the periselenium of the osculating orbit, it crosses again the plane $p(\vartheta)$ with negative or zero Keplerian energy with respect to m_2 without going around m_1.

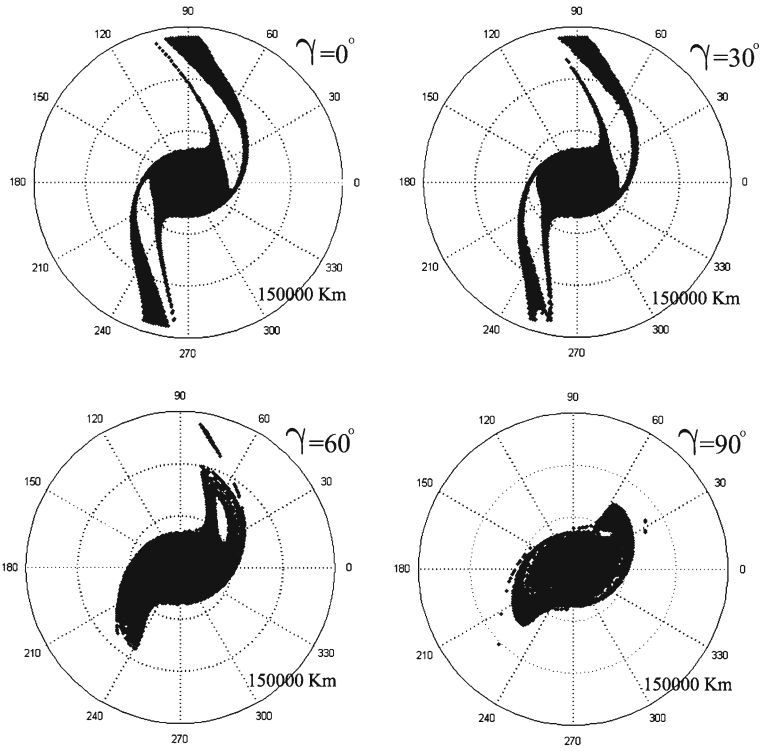

Fig. 16 WSB structure for increasing values of γ with $e = 0$ in the framework of the CRTBP

On the contrary, the motion of the third body is unstable if:

- after a complete revolution around m_2, it crosses again the plane $p(\vartheta)$ without going about m_1 but with a positive Keplerian energy with respect to m_2;
- after leaving the plane $p(\vartheta)$, the third body moves away from m_2 towards m_1 and makes a cycle about m_1 without crossing anymore the plane $p(\vartheta)$ or it collides with m_1.

As in the planar case it is necessary to search for the values of the radius $r^* = r^*(\vartheta, e, \gamma)$ corresponding to stable/unstable transitions, and vice versa. The definition of the WSB is then extended to the three-dimensional case as:

$$W = \left\{ r^*(\vartheta, e, \gamma) \in R^1 \,\middle|\, \vartheta \in [0, 2\pi], e \in [0, 1), \gamma \in [0, 2\pi] \right\} \tag{8}$$

Figure 16 shows the configuration of the WSB for different values of the angle γ in the framework of the CRTBP with initial eccentricity of the osculating orbit $e = 0$.

As illustrated, for increasing values of the out of plane angle γ, the structure of the WSB changes remarkably reducing the extension of the capture zone. Note that the arms, typical for low values of the angle γ, tend to join together at the ends, shrink and form a single structure. If the satellite eccentricity gains a higher value $e = 0.92$, which is typical value for translunar low–energy transfers, the WSB structure changes as illustrated in Fig. 17.

It is clearly seen that, in general, for high values of the eccentricity the extension of the stable zone is reduced and for increasing values of the angle γ the number of stable points decreases enormously. Particularly, for $\gamma = 90°$, that is for polar initial conditions, the WSB

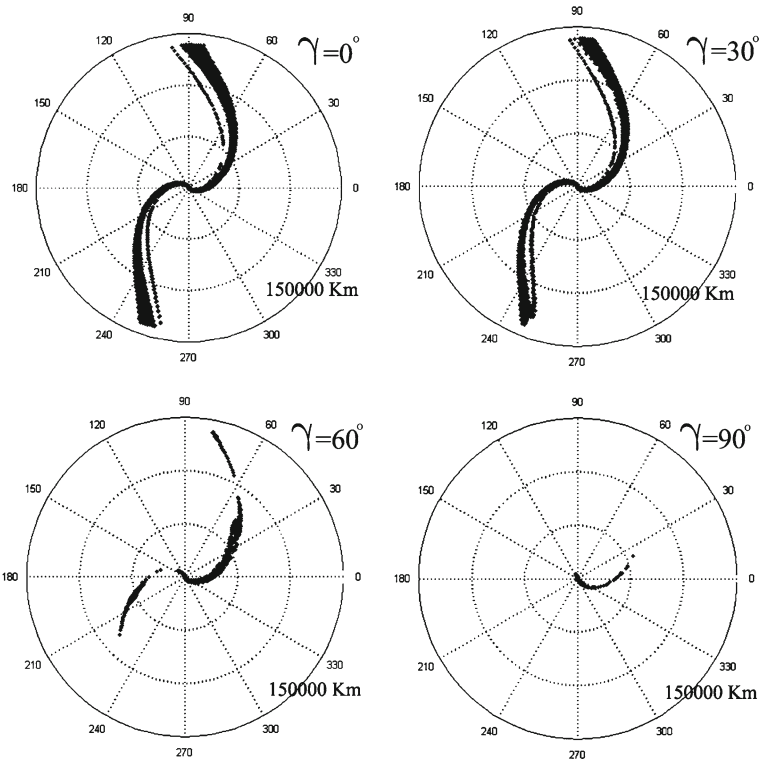

Fig. 17 WSB structure for increasing values of γ and $e = 0.92$ in the framework of the CRTBP

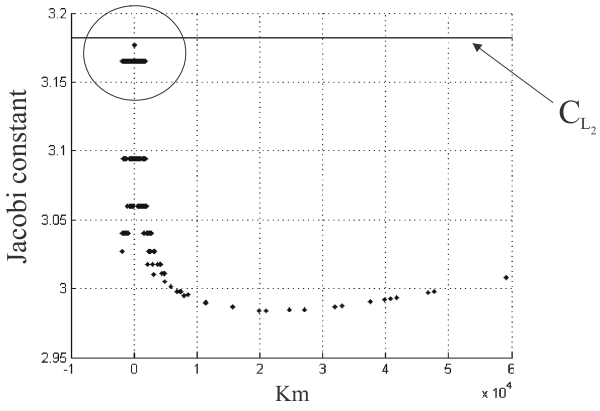

Fig. 18 Jacobi constant for stable points with $\gamma = 90°$ and $e = 0.92$

are reduced to a very small structure close to the Moon. Figure 18 shows the Jacobi constant values for the case $e = 0.92$ and $\gamma = 90°$.

Note that the Jacobi constant values are all below the value $C_{L_2} = 3.1722$ and, therefore, the zero velocity curves are fully opened. Particularly, the Jacobi constant is almost equal to C_{L_2} for the points close to the Moon, which correspond to points close to the origin of the x axis in Fig. 16. Hence, these points lead to minimum energy transfer conditions, that is the

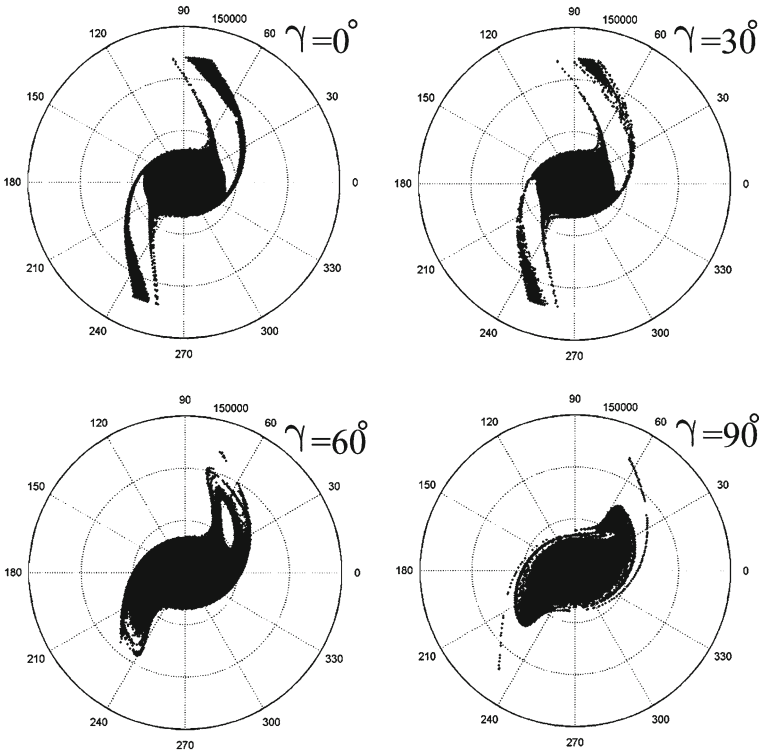

Fig. 19 WSB structure for increasing values of γ and $e = 0$ in the BRFBP

zero velocity curves are as open as strictly necessary to allow the passing of the spacecraft. The same procedure can be repeated using the elliptic three body problem and the bicircular four body problem. Numerical simulations showed that the results are similar to those obtained in the framework of the CRTBP and differences appear only with a zoom of the region considered (Figs. 19, 20).

Comparing Figs. 19 and 20 against Figs. 16 and 17 it is immediately seen that there are slight differences between the two cases. Particularly, the presence of the Sun slightly increases the extension of the WSB, especially with high values of the out of plane angle γ and of the eccentricity e of the osculating initial orbit. It is important to note that this slight dependency of the WSB to the perturbations acting on the Earth–Moon system has not to be confused with the great importance that these perturbations have on the dynamics of low-energy lunar transfers. From the point of view of the WSB definition, that is from the point of view of the identification of the stable/unstable transition conditions, the influence of the eccentricity of the Moon around the Earth and of the Sun gravitational effect is in first approximation negligible. The three-dimensional case can be further extended introducing an angle δ (Fig. 21), which represents a rotation of the plane $p\,(\gamma)$ around the z axis of the synodic reference frame. The structure of the WSB is, then, investigated after a rotation γ around the x axis and a rotation δ around the z axis.

Assuming $\delta \in [0°\ 90°]$ and $\gamma = 90°$, that is only polar initial conditions for the third body are considered, the plane $p(\gamma)$ will pass from the $(z - x)$ reference plane to being parallel to

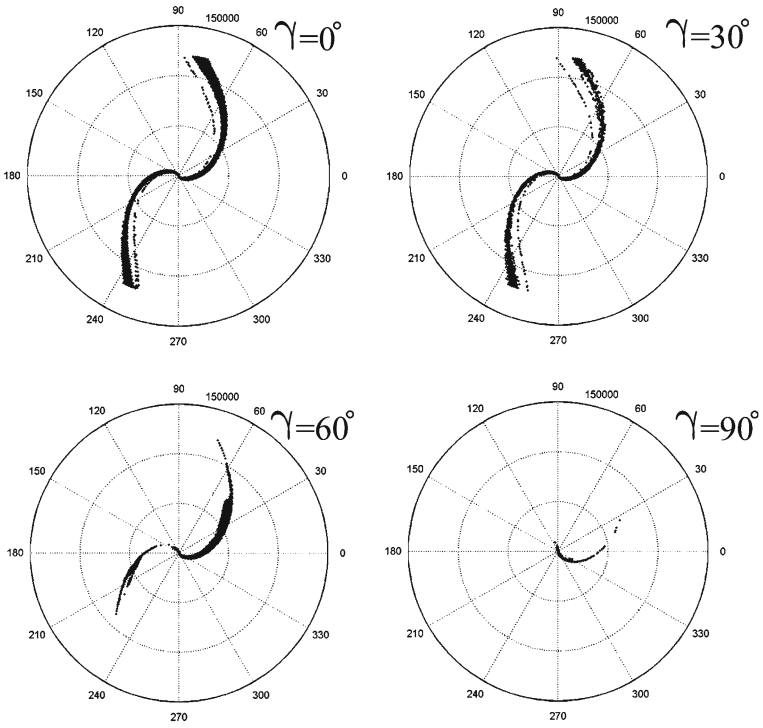

Fig. 20 WSB structure for increasing values of γ and $e = 0.92$ in the BRFBP

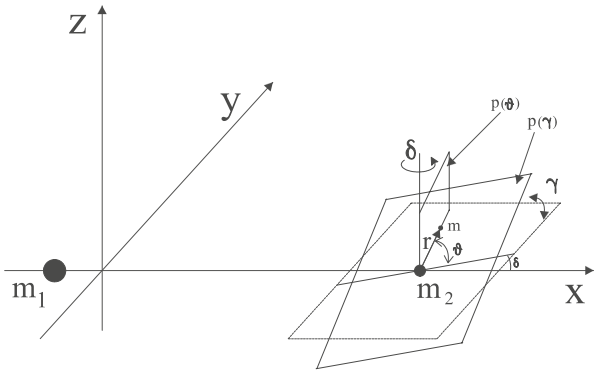

Fig. 21 Rotation of the plane $p(\gamma)$ around the z axis

the $(z - y)$ reference plane. Figure 22 shows the geometry of the WSB for different values of the angle δ and high values of the initial osculating orbit eccentricity ($e = 0.92$).

As illustrated, first the extension of the capture zone rises, then decreases for initial conditions corresponding to the plane $p(\gamma)$ normal to the Earth–Moon direction ($\delta = 90°$).

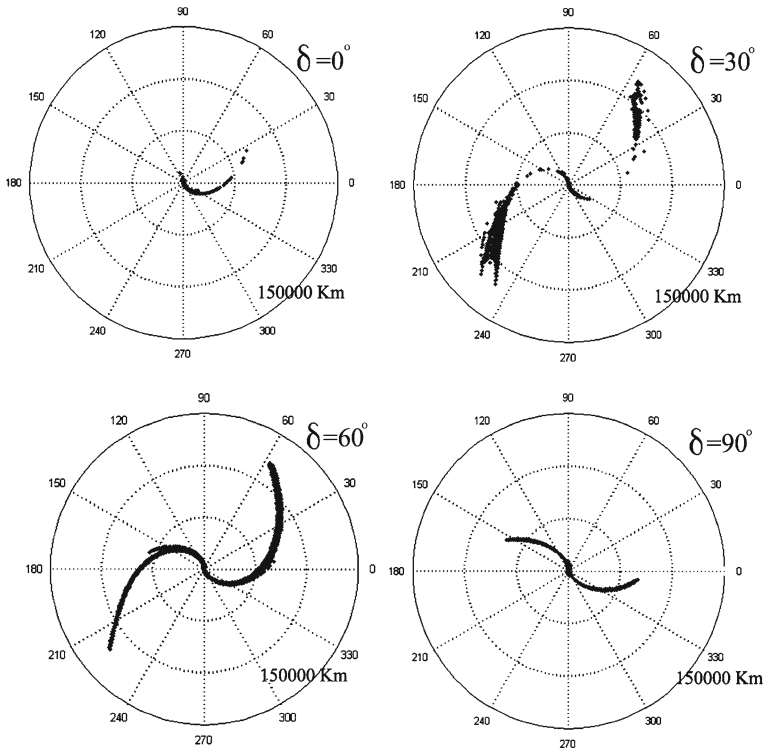

Fig. 22 WSB structure for increasing values of the angle δ with $e = 0.92$ and $\gamma = 90°$

5 Trajectories evolution after capture

Information about the stable/unstable feature of motion for a point in the Earth–Moon system is important for the trajectory design, but another fundamental parameter is the minimum periselenium altitude. The knowledge of this quantity, in fact, is very useful to design safe capture orbits and avoid impacts with the surface of the Moon. Hence, it is possible to study the trajectory evolution of the third body and determine the minimum distance from m_2. Generally, three different cases are possible:

(i) The third body reaches a positive periselenium altitude greater than the initial height;
(ii) The third body reaches a positive periselenium altitude smaller than the initial height;
(iii) The third body reaches a negative periselenium altitude, that is the spacecraft collides with the lunar surface.

First of all, it is important to distinguish between the couples of values (r, ϑ) that lead to a safe flyover of the lunar surface and those that, on the contrary, lead to impacts with the surface. Note that both the value of the angle γ and the eccentricity of the initial osculating orbit are parameters that strongly affect the safe/unsafe characteristic of motion. Numerical simulations executed with the circular, elliptic and bicircular models showed similar results. Hence, only the bicircular four body model results will be illustrated. Figure 23 shows the results with $e = 0.92$ and an integration time of 30 days.

For increasing values of the out of plane angle γ, the number of stable points decreases as previously said. Nevertheless, for each value of γ, points that avoid collisions with the lunar

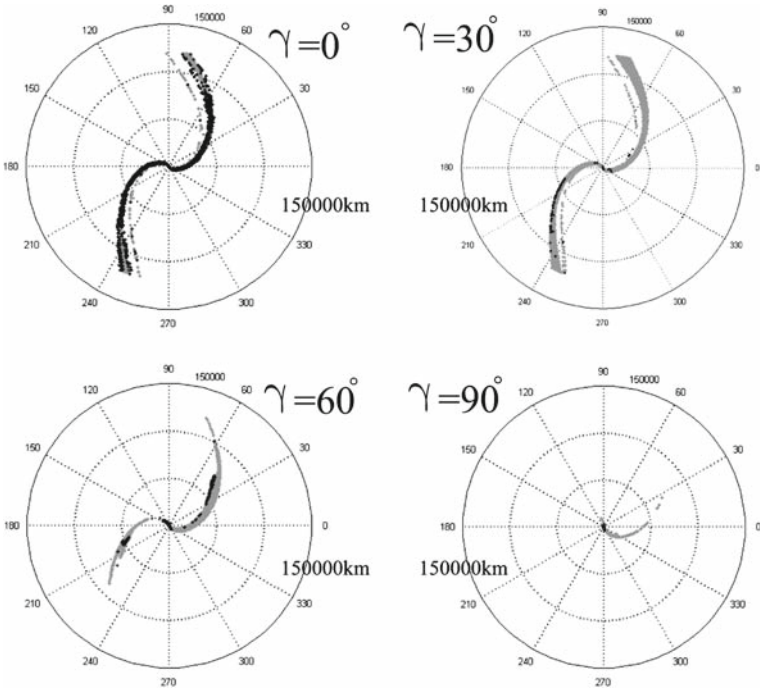

Fig. 23 Safe conditions (gray points) and impacts conditions (black points) for increasing values of γ and $e = 0.92$

surface exist (gray points in Fig. 23) as well as conditions that lead to a collision with the lunar surface (black points in Fig. 23). Particularly, it is clearly seen that, as γ increases, the ratio between the number of stable and safe points with the number of stable points increases. Note that the black points in left high corner of Fig. 23 are due to a superimposition of both safe and unsafe conditions very close one to each other: for equatorial orbits ($\gamma = 0°$), the number of stable and safe conditions is approximately the same as the number of stable and unsafe conditions. For polar conditions, then, it is more difficult to obtain stable orbits than in the equatorial case, but the possible orbits are more probably safe. Besides, it must be specified that for polar orbits the region close to the Moon presents both safe and unsafe points, with the safe ones located along the Earth–Moon direction. Finally, for a fixed value of the angle $\gamma = 90°$ it is possible to investigate the evolution of motion for increasing values of the angle δ in the definition range $[0°, 90°]$. Integrating the equations of motion for a 30 days time interval, the results in Fig. 24 are obtained.

As in the previous case, the region close to the Moon, which corresponds to low altitude orbits, includes unsafe and safe points.

6 WSB and lunar low-energy transfers

Lunar WSB information can be used to design lunar transfers with stable capture. In this way, it is possible to execute the circularization maneuver even after the first periselenium passage or to have the required time to stabilize the trajectory with low-thrust propulsion systems. Lunar low-energy transfers use the Earth–Sun WSB, in order to obtain a first ΔV to raise the perigee to the lunar height, and Earth–Moon WSB to reach capture with the minimum

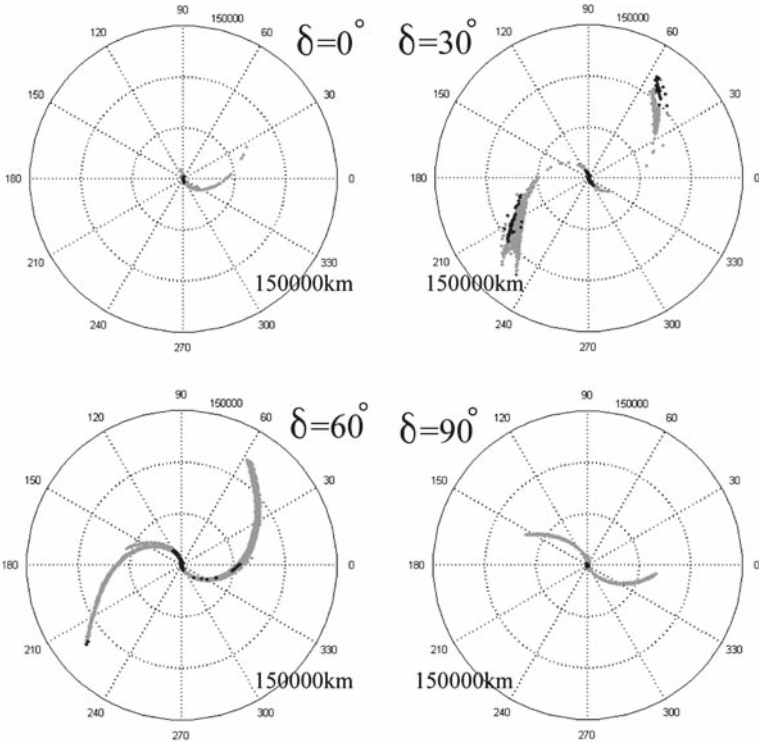

Fig. 24 WSB safe zone for increasing values of the angle δ and $\gamma = 90^\circ$ (gray points)

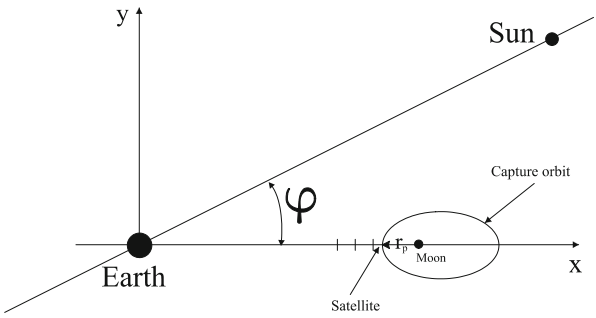

Fig. 25 Capture conditions for WSB lunar transfers

amount of energy. These transfers require a fine synchronization between the position of the Moon and that of the Sun at the beginning of the transfer. These transfers are usually studied to reach a low altitude periselenium of about 200 km with an extremely high capture eccentricity of about $e = 0.92$ (Bellò et al. 2000; Circi et al. 2000). However, it is possible to obtain low-energy transfers with eccentricity smaller than $e = 0.92$, raising the satellite pericenter altitude r_p along the Earth–Moon direction (Fig. 25), reducing in this way the total ΔV required for the mission.

Figure 26 shows the performances of the lunar WSB transfers, obtained using the bicircular four body model. Note that small disks correspond to transfers with equatorial captures, while crosses represent polar captures.

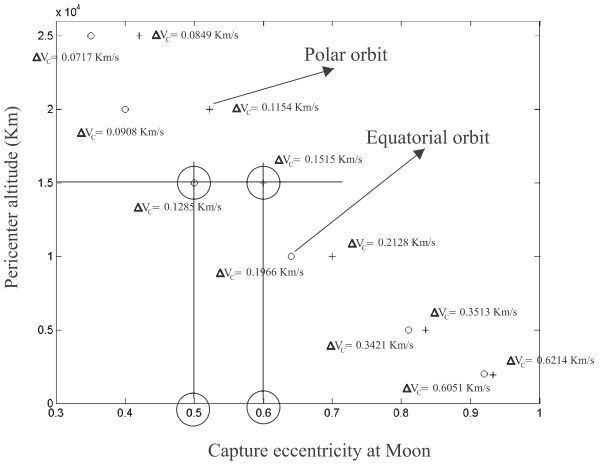

Fig. 26 Performances for low-energy transfers in terms of r_p and e

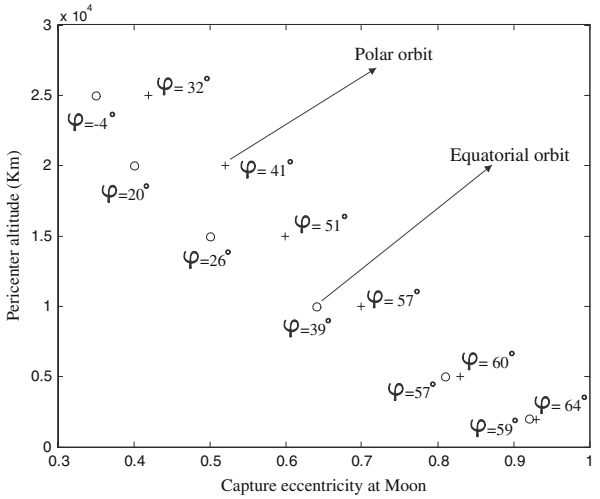

Fig. 27 Initial phase angle φ for low-energy transfers in the BRFBP

Transfer time varies between 90 and 100 days, while the ΔV_c for the circularization maneuver decreases considerably as the pericenter rises. As illustrated, for a fixed value of the pericenter altitude, equatorial captures lead to smaller values of the eccentricity and, therefore, to smaller values of the ΔV_c for circularization. Figure 27 shows the initial conditions for the phase angle φ (Fig. 23), used for the transfers of Fig. 26.

Figure 28 shows the Jacobi constant value (C) for the satellites during the transfers illustrated in Fig. 26.

Note that the value of C is not constant due to the presence of the Sun. It is easily seen that the transfers with equatorial capture have a greater value of C, hence equatorial captures happen with a lower amount of energy than polar captures. Besides, for the same family of capture, it is evident that the value of C rises for decreasing values of the periselenium altitude and for increasing values of the capture eccentricity. This stresses how transfers with low pericenter altitude and high capture eccentricity give the best results in terms of capture. Figure 29 shows different capture trajectories for lunar WSB transfers.

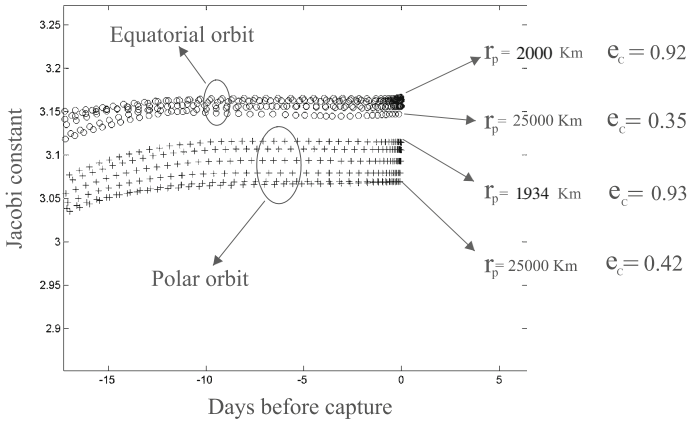

Fig. 28 Jacobi constant on low-energy trajectories

Fig. 29 Polar and equatorial captures for WSB lunar transfers

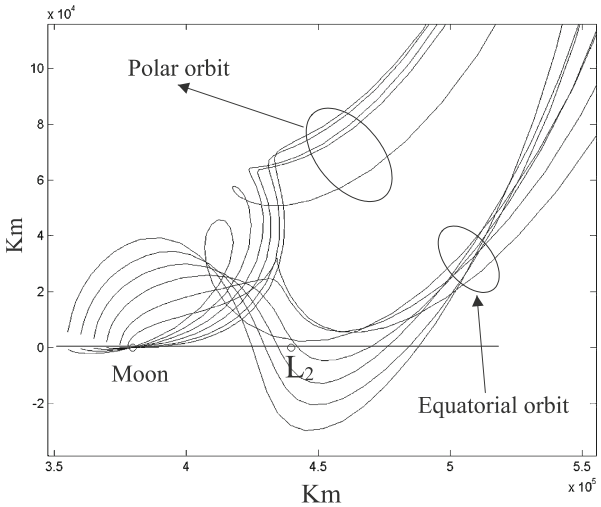

As illustrated, the two families of curves are easily distinguishable. In particular, it is evident that equatorial captures happen with high values of the Jacobi constant and, therefore, capture occurs in the vicinity of the L_2 libration point, with a small opening of the zero velocity curves.

In order to execute the circularization maneuver with low-thrust propulsion systems, it is recommended that a stable capture in the WSB be obtained. Assuming that the desired periselenium altitude is 15,000 km along the Earth–Moon line direction, Fig. 26 shows that, for equatorial captures, the transfer must have a capture eccentricity of $e = 0.5$. Once the WSB geometry is known, it is possible to determine if the capture orbit is stable or unstable, that is if the spacecraft will cross the radial line $l\ (\vartheta)$ again performing a complete revolution around the Moon. Figure 30 shows the structure of the WSB with $e = 0.5$.

As illustrated in Fig. 30, the selected point is out of the stable zone and, therefore, the circularization maneuver has to be executed at the first periselenium passage. In this way, it is not possible to take advantage of stable motion, which ensures that the spacecraft per-

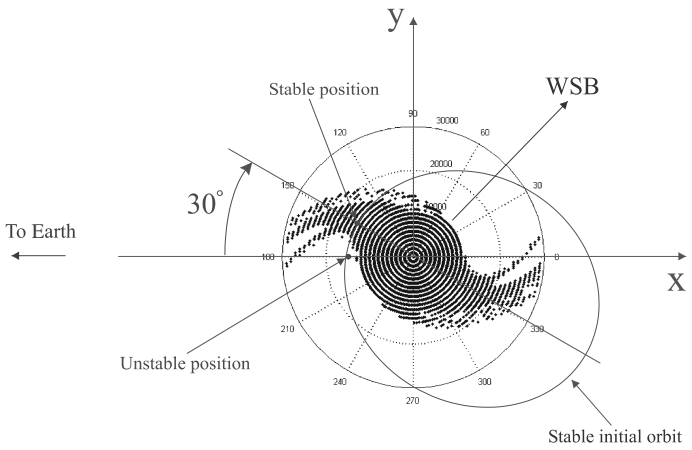

Fig. 30 WSB structure for equatorial orbits and eccentricity capture $e = 0.5$

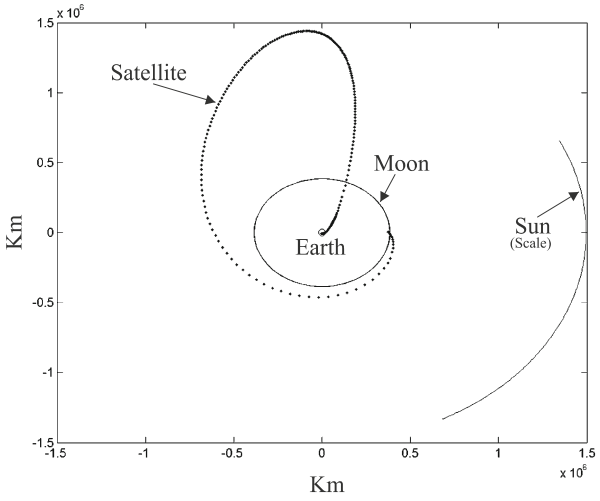

Fig. 31 WSB lunar transfer with stable capture orbit

forms at least one complete revolution around the Moon. This means that, if the motion of the spacecraft is integrated forward in time from these conditions out of the stable region, the trajectory will be unstable and an escape towards the L_1 Lagrangian point will occur, in agreement with Sect. 2. Note that if the line of apsides of the capture orbit is rotated by 30°, the initially unstable point enters the stable region and, therefore, once the motion is integrated forward in time from these new conditions the spacecraft performs at least one complete revolution of the Moon. Hence, it is important to distinguish the dynamics of the motion of the spacecraft before and after the capture. Figure 31 shows the lunar transfer made with the new geometry obtained after the rotation of 30° of the line of apsides.

The new transfer geometry ensures stable capture conditions. Although the capture eccentricity for the new conditions decreases from $e = 0.5$ to $e = 0.48$, changes in the geometry of the WSB are negligible and the satellite is captured with stable conditions. In the case of polar captures, in order to obtain a periselenium altitude of 15,000 km a capture eccentricity

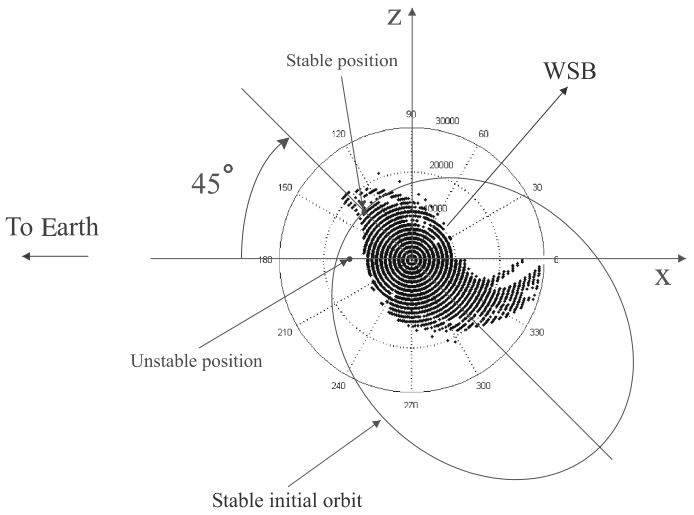

Fig. 32 WSB structure for polar orbits with capture eccentricity $e = 0.6$

Fig. 33 WSB lunar transfer with stable capture orbit

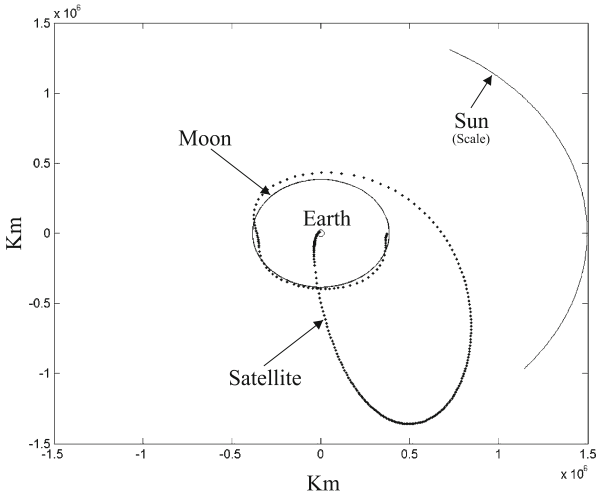

$e = 0.6$ is needed (Fig. 26). Figure 32 shows the associated WSB structure. It is easily seen that the spacecraft is in the unstable region.

As mentioned for the equatorial case, it is possible to rotate the line of apsides by 45° in order to obtain a new geometry which leads to stable capture conditions. Figure 33 shows the transfer associated with the new configuration.

Note that in order to realize the designed transfer, the capture eccentricity increases from $e = 0.6$ to $e = 0.62$ but, as in the previous case, the related changes in the WSB structure are negligible and, therefore, the spacecraft is in the stable region.

7 Conclusion

The structure of the lunar WSB has been investigated using both the three and four body models, in the plane and in the three-dimensional cases. Single and multiple stable/unstable transitions have been considered to find the WSB for increasing values of the periselenium altitude of the initial osculating orbit of the spacecraft. In the case of multiple transitions it has been stressed that the extension of the capture zone is enlarged with respect to the single transition definition, with the presence of four arms along the direction normal to the Earth–Moon line. This behavior can be related to the action of the Earth gravity-gradient, which removes or provides energy to the spacecraft and makes the motion stable or unstable, respectively. For different values of the initial orbit eccentricity around the Moon, numerical simulations showed that for increasing values of eccentricity the extension of the stable zone decreases and becomes closer to the Moon, while the over all dimension of the arms remains approximately the same. The analytical approximation based on the value of the Jacobi constant, is very close to the numerical solution with one single transition. In fact, in this case the information about the presence of the arms is totally lost. The influence of the lunar orbit eccentricity and of the presence of the Sun does not affect a lot the WSB geometry, both in the planar and in the three-dimensional case. The trajectory evolution after capture allowed us to determine stable and safe trajectories, that is stable trajectories that avoid impacts with the lunar surface. This study illustrated that stable polar captures are less in number compared with the equatorial case but, at the same time, polar captures decrease the possibility of collisions with the surface. Lunar low-energy transfers' geometry and performance, in terms of the ΔV_c required for the circularization maneuver, have been studied in the framework of the bicircular four body problem for different values of the pericenter altitude. It has been shown that equatorial captures with low pericenter altitude lead to minimum energy transfers. Finally, the information about the structure of the WSB allowed us to design lunar low-energy transfers with stable capture orbits.

References

Belbruno, E.: Lunar capture orbits, a method for constructing Earth–Moon trajectories and the lunar GAS mission. In: Proceedings of AIAA/DGLR/JSASS Inter. Propl. Conf. AIAA Paper No. 87-1054 (1987)

Belbruno, E.: Capture Dynamics and Chaotic Motions in Celestial Mechanics. pp. 144–148. Princeton University Press, Princeton (2004)

Belbruno, E., Miller, J.K.: A ballistic lunar capture trajectory for the Japanese spacecraft hiten. Jet Propulsion Laboratory, IOM 312/90.4-1371-EAB (1990)

Belbruno, E., Miller, A., James, K.: Sun perturbed Earth-to-moon transfers with ballistic capture. J. Guidance Control Dyn. **16**(4), 770–775 (1993)

Bellò, M., Graziani, F., Teofilatto, P., Circi, C., Porfilio, M., Hechler, M.: A systematic analysis on weak stability boundary transfers to the moon. In: 51st International Astronautical Congress, Paper No. IAF-00-A.6.03 (2000)

Circi, C., Teofilatto, P.: On the dynamics of Weak Stability Boundary Lunar transfers. Celest. Mech. Dyn. Astron. **79**(1), 41–72 (2001)

Circi, C., Graziani, F., Porfilio, M., Teofilatto, P.: Weak Stability Boundary lunar transfers from Soyouz and Rockot planar launches. In: Proceedings of the 22nd International Symposium on Space Technology and Science, Paper No. ISTS 2000-j-01, pp. 1555–1563, Morioka (2000)

Garcia, F., Gomez, G.: A note on weak stability boundaries. Celestial Mech. Dyn. Astr **97**(2), 87–100 (2007)

Kawaguchi, J., Yamakawa, H., Uesugi, T., Matsuo, H.: On making use of lunar and solar gravity assist for Lunar A and planet B missions. Acta Astronautica **35**, 633–642 (1995)

Koon, W., Lo, M., Marsden, J., Ross, S.: Heteroclinic connections between Lyapunov orbits and resonance transitions in celestial mechanics. Chaos **10**, 427–469 (2000)

Koon, W., Lo, M., Marsden, J., Ross, S.: Low energy transfer to the Moon. Celest. Mech. Dyn. Astron. **81**(1), 63–73 (2001)
Szebehely, V.: Theory of Orbits. Academic Press, New York (1967)
Yagasaki, K.: Sun-perturbed Earth-to-Moon transfers with low energy and moderate flight time. Celest. Mech. Dyn. Astron. **90**(3/4), 197–212 (2004)
Wie, B.: Space Vehicle Dynamics and Control. Published by AIAA 1998, AIAA Education Series (2000)